Theoretical Chemistry Accounts (2025) 144:67
https://doi.org/10.1007/s00214-025-03225-1

RESEARCH

Exploring of a potential energy surface around a valley bifurcation

Wolfgang Quapp[1] · **Grace Hsiao-Han Chuang**[2] · **Josep Maria Bofill**[3,4]

Received: 25 March 2025 / Accepted: 2 July 2025

Abstract
Valley-ridge inflection (VRI) points play an important role in organic chemistry, especially in post-TS bifurcations. We explain a new discovery of a special structure of the region with another, weaker type of a valley bifurcation (VB) without a ridge in between. We apply the theory of Newton trajectories (NTs) and gradient extremals (GEs) to cases of two-dimensional potential energy surfaces. We define an indicator of the valley bifurcation where the gradient of the potential energy surface is the eigenvector of the Hessian matrix at eigenvalue zero. The new type of bifurcation point is connected with a 'dead' valley of the PES. The example is a nice demonstration that the index theorem for NTs holds, nevertheless. NTs and GEs are important tools to explore the region of the bifurcation point.

Keywords Potential energy surface · Transition state · Valley-ridge inflection point · Valley bifurcation · Regular and singular Newton trajectory · Gradient extremal

1 Introduction

Bifurcations are omnipresent in natural sciences [1, 2], including valleys on a potential energy surface (PES). They are a long studied subject [3–8]. The bifurcation can take place before the transition state (TS) of a dissociation [9, 10], as it is demonstrated by an internal vibrational redistribution [11]. It also can happen at the TS [12, 13]. Or in contrast, the study of organic chemical reactions shows often bifurcations after the first TS. The theoretical understanding of the underlying mechanisms that govern selectivity, i.e., product distributions, is of central interest [14–19]. And finally, the bifurcation can coalesce with a TS [6, 20]. Bifurcations can also take place in radiationless deactivation of organic dyes on the lower PES [21].

Understanding in particular asymmetric post-transition state bifurcations is essential for predicting reaction selectivity in complex chemical systems [22, 23]. Of course, here the reaction pathways inherently require at least a two-dimensional (2D) description, as long as a pathway over a single transition state bifurcates into two distinct product pathways. The PES has two consecutive saddles of index 1 with no intervening energy minimum. Between the two index 1 saddles, one of which has higher energy than the other, there must be a valley ridge inflection (VRI) point [6, 24–28].

The reaction is initiated when a trajectory crosses the area of the higher saddle (forming the entrance channel) and may approach the lower energy saddle. On either side of the lower energy saddle, there are two minimum wells. The question of interest is which well does the trajectory enter (predicting the product selectivity)? It could leave the standard intrinsic reaction path, the IRC [29–32].

One can assume that the VRI plays a role in selectivity. Certainly the VRI is a geometrical feature of the PES. Two conditions are fulfilled there: The curvature of the PES is zero, which implies that the Hessian matrix has a zero

✉ Wolfgang Quapp
quapp@math.uni-leipzig.de

Grace Hsiao-Han Chuang
hhchuang@pks.mpg.de

Josep Maria Bofill
jmbofill@ub.edu

[1] Mathematisches Institut, Universität Leipzig, Augustus-Platz PF 100920, D-04009 Leipzig, Germany

[2] Physics of Complex Systems, Max Planck Institute, Noethnitzer Str. 38, D-01187 Dresden, Germany

[3] Química Inorgànica i Orgànica, Secció de Química Orgànica, Universitat de Barcelona, Martí i Franquès 1, 08028 Barcelona, Catalunya, Spain

[4] Institut de Química Teòrica i Computacional (IQTCUB), Universitat de Barcelona, Martí i Franquès 1, 08028 Barcelona, Catalunya, Spain

Published online: 16 July 2025

eigenvalue, and the gradient of the potential is perpendicular to the eigenvector corresponding to the zero eigenvalue. This means that the landscape of the PES in the neighborhood of the VRI changes its shape from a valley to a ridge which gave the region the name VRI.

In synthetic chemistry, identifying the key functional groups that influence reaction pathways is crucial for designing efficient synthesis strategies, especially when dealing with large molecules containing multiple functional groups. If the dominant degrees of freedom are known, especially the VRI region, chemists can target these features to streamline synthesis.

In this paper, we analyze cases where a valley bifurcation occurs without an intervening ridge. We call this event valley bifurcation (VB). In the next section, we repeat the definition of the reaction path models of interest: Newton trajectories (NTs) and gradient extremals (GEs). In Section III, we discuss different relations of a VRI region to the singular NT traversing it, and of cases of onyl VB, for different 2D test PES. In Section VI, we add a discussion. A conclusion is given in Section V. Appendix 1–3 reports on the index theorem of NTs, the avoided crossing of GEs, and the 2D representation of NTs or GEs.

2 Models of the reaction path

2.1 Newton trajectory

This work concerns a mathematical excursion which discusses the use of NTs for the exploration of a special PES, $V(\mathbf{x})$ given in reference [33], and in particular its VRI or VB points. An NT is a curve $\mathbf{x}(t)$ where the gradient, $\mathbf{g}$, of the PES is parallel to a given direction, $\mathbf{f}$, at every point

$$\mathbf{g}(\mathbf{x}(t)) \quad || \quad \mathbf{f} \tag{1}$$

t is a curve length parameter. Curves that solve Eq.(1) are of particular interest in mechanochemistry, where the direction $\mathbf{f}$ is the direction of an external force [34–36]. A possibility to follow a curve fulfilling this property (1) is the definition of a projector matrix. If $\mathbf{r} = \mathbf{f}/|\mathbf{f}|$ is the normalized direction then

$$\mathbf{P} = (\mathbf{I} - \mathbf{r}\mathbf{r}^T)$$

projects on direction $\mathbf{r}$. Eq.(1) looks then

$$\mathbf{P}\,\mathbf{g}(\mathbf{x}(t)) = \mathbf{0}\,.$$

Its derivation can be used to develop a predictor-corrector method [6].

Alternatively, the approach of Eq.(1) was formulated in a differential equation by Branin [6, 37, 38]

$$\frac{d\mathbf{x}(t)}{dt} = \pm Det(\mathbf{H}(\mathbf{x}(t)))\ \mathbf{H}^{-1}(\mathbf{x}(t))\,\mathbf{g}(\mathbf{x}(t)) \tag{2}$$

$\mathbf{H}$ is the Hessian of the second derivatives of the PES. It is important that the matrix

$$\mathbf{A} = Det(\mathbf{H})\ \mathbf{H}^{-1} \tag{3}$$

is desingularized when the Hessian becomes singular. It is called the adjoint matrix for $\mathbf{H}$. The full Hessian matrix can be computationally expensive at each step of the positions $\mathbf{x}(t)$. However, it can be updated [39–41]. A first numerical step starts from a stationary point in direction $\mathbf{f}$. The following steps then ensure that the gradient maintains this direction [6]. The plus + sign in Eq. (2) is used for an NT from a minimum to an SP of index one, but the minus - vice versa. If the energy increases monotonically along an NT, then it can serve for a reaction path variable.

Note that NTs have the nice property that they connect stationary points with an index difference of one [6, 38, 42], compare appendix 1. The index here counts the number of negative eigenvalues of the Hessian matrix at the stationary point. If we start at a minimum with index zero, we obtain a next saddle point (SP) with index one. A special case is a singular NT that crosses a valley ridge inflection (VRI) point [6]. The characterization of the VRI is the zero point of the right-hand side of the Branin Eq. (2)

$$\mathbf{A}\,\mathbf{g} = \mathbf{0} \tag{4}$$

but where the gradient is not zero, $\mathbf{g}(\mathbf{x}) \neq \mathbf{0}$. We call it VRI point. A singular NT has four branches through the VRI point. It typically connects a minimum with a saddle of index two and two SPs of index one via the VRI. A VRI represents the branching of a valley into two valleys and an intermediate ridge, or complementarily, the branching of a ridge into two ridges and a valley in between. Mathematically, the Hessian has a zero eigenvector orthogonal to the gradient [6, 8, 31, 43, 44].

We can follow a one-dimensional curve by Eq. (2) in any dimension. For a PES with more than two dimensions, manifolds of VRI points arise [45, 46]. There is an illustrative introduction to the higher dimensional case [47]. The following of an NT is included in the COLUMBUS program system [48] (under the name reduced gradient following, RGF). There are some links to different programs [49, 50]. If the PES is symmetric, the VRI manifold often forms a symmetry hypersurface. However, asymmetric VRI manifolds can also be computed [45, 49, 51, 52]. Recently, the role of VRI points in dynamical processes has been discussed [53]. The Newton trajectory method has been established in chemistry since 1998, see refs. [36, 54–59] and further references therein. We report that NTs are calculated for medium molecules with up to dimension 486 [60].

2.2 Gradient extremal

A second kind of curves which also can serve for the description of reaction valleys are gradient extremals (GE) [6, 61–64] where holds

$$\mathbf{H}(\mathbf{x}(t))\mathbf{g}(\mathbf{x}(t)) = \lambda\, \mathbf{g}(\mathbf{x}(t)) \tag{5}$$

thus on a GE the gradient, **g**, is an eigenvector of the Hessian, **H**, with (varying) eigenvalue λ. GEs are represented in the following figures by black dashed curves. A VRI point is crossed by a GE if the pseudo-convexity index μ [65, 66] changes its sign

$$\mu = \frac{\mathbf{g}^T\, \mathbf{A}\, \mathbf{g}}{\mathbf{g}^T\, \mathbf{g}} \tag{6}$$

Below we explain a new type of a valley bifurcation (VB) region by the crossing of a GE with an index boundary line, Eq. (7). Then the condition (6) does not apply.

GEs can bifurcate itself [62, 63, 67]. This happens when the two eigenvalues, λ in Eq. (5), of the two intersecting branches become equal. Normally, however, these two equal eigenvalues are not zero. Therefor, no VRI point is indicated by such a crossing. But the GE crossing can indicate the change of a valley ground into a circle [67]. Then the bifurcation of the GE can be an indication on a nearby VB or VRI event. A pitch fork GE is, in a sense, a preview to a VB or a VRI point. On an asymmetric PES, however, the normal case is the avoided crossing of the GEs. We report an example in appendix 2.

Typically, N GEs emanate from a stationary point, if N is the dimension of the PES. Then the GE to the smallest eigenvalue λ_{min} describes the baseline of the reaction valley. This GE can be considered a static representation of a reaction path.

2.3 Index boundary

Another interesting type of curves is the boundary between regions of a different index of the Hessian of the PES. For the case of 2D surfaces $V(x, y)$, they are given by

$$Det(\mathbf{H}) = V_{xx}\, V_{yy} - V_{xy}^2 \;\; = \;\; 0 \tag{7}$$

and these index boundaries (IB) are represented by thin green curves in the following figures.

3 2D example PES

A series of PES is used of Ref. [33]

$$V(x, y) = x^4 - 2x^2 + y^4 + y^2 - 1.5x^2y^2 + x^2y - c\, y^3 \tag{8}$$

as shown in the following figures. The constant c is a parameter that varies here between 1 and 2.

3.1 PES for c=1.5

First, we discuss a 'normal' case for parameter c=1.5 of PES (8). One can observe in Fig. 1 that the right valley from M_1 to M_2 bifurcates to the SP_{top}. There are only stationary points of index zero, minima, and of index one, transition states (TS). By different curves, we can determine the exact VRI point. This is demonstrated in Fig. 1B. Here the 4 branches of the singular red NT intersect at the VRI. The search direction of the singular NT is $\mathbf{f}_{red}$=(−1.3, 0.33). It is the gradient at the solution of Eq. (4). The VRI is at (x, y)=(0.47, 0.23) with

$\mathbf{g} = \begin{pmatrix} -1.32 \\ 0.34 \end{pmatrix}$, $\mathbf{H} = \begin{pmatrix} -1.13 & 0.29 \\ 0.29 & -0.07 \end{pmatrix}$ and $\mathbf{A} = \begin{pmatrix} -0.07 & -0.29 \\ -0.29 & -1.13 \end{pmatrix}$.

The vector with Eq. (4) is $\mathbf{A}\,\mathbf{g} = \mathbf{0}$; thus, the gradient is the zero eigenvector of **A**, and the second eigenvalue is

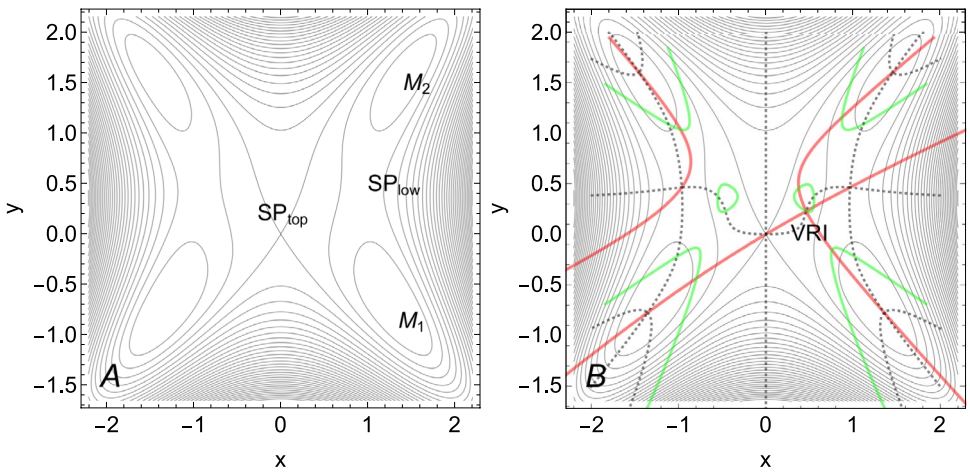

Fig. 1 A: Level lines of PES (8) for c=1.5. The axis x=0 is an axis of symmetry. M_1 is a minimum, SP_{low} is the transition state to the minimum M_2. The global SP_{top} lies central on the y axis at point (0, 0). B: A VRI point is located between SP*top* and the stationary points in the valley on the right-hand side. Three types of curves are shown: Bold red is the singular NT through the right VRI point, GE curves are dashed black, and the IB lines are thin green

$\lambda = -1.204$ being the eigenvalue of the matrix **H** for the eigenvector **g**. The vector

$\mathbf{v} = \begin{pmatrix} 0.34 \\ 1.32 \end{pmatrix}$

is then the zero eigenvector of the Hessian orthogonally to the gradient. It is the characteristic of the VRI point. Note that Hessian and adjoint Hessian have the same eigenvectors, but for the eigenvalues λ_i of the Hessian and μ_i of the adjoint the following applies for every i [68, 69]

$$\mu_i \, \lambda_i \; = \; Det(\mathbf{H}) \; = \; \prod_{k=1}^{N} \lambda_k \tag{9}$$

For $N = 2$ it means $\mu_1 = \lambda_2, \;\; \mu_2 = \lambda_1$.

A thin green border line of Det(**H**) crosses a GE there. Thus, all three curves cross at the VRI point. (The calculation of these curves is described in appendix 3.) The boundaries of the different Det(**H**) regions are given by the condition of Eq. (7). Normally they are curvilinear, so that the points of a molecule on a higher dimensional PES with the IB condition $Det(\mathbf{H}) = 0$ form curved hypersurfaces.

The VRI is intersected by its own singular NT which is represented by the bold red lines. The four branches form an almost orthogonal cross at the VRI point. This is the long known type of a valley bifurcation. Singular NTs are the boundaries of families of NTs that connect the minimums, M_i, to different *SPs*. Any two neighboring branches of the singular NT form a corridor for all NTs connecting a given minimum, *M*, with the same *SPi* [70]. The stationary points are also crossed by the NT and by the various branches of the GEs.

In Fig. 2, the vector field of the right-hand side of the Branin Eq. (2) is included on the PES with c=1.5. The hyperbolic touching of the corresponding NTs before and after the VRI point is a characterization of this region.

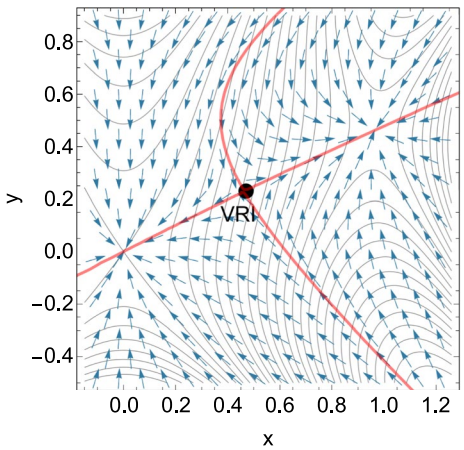

Fig. 2 Vector field of the Branin Eq. (2) with plus sign on a section of the PES of Fig. 1. The VRI point is characterized by the hyperbolic touching of the corresponding regular NTs

3.2 PES for c=1

A 3D representation of this PES is shown in Fig. 3. Here we develop the case of interest for a VB with a nonsingular NT, because a singular NT is missing, but a GE is included again.

One can observe in Fig. 4 that the right valley from M_1=M uphill to the right-hand side bifurcates again to a valley to the $SP_{top} = SP$, the only SP which remains. There is also a thin green border line, as well as a GE which crosses it. The gradient is the eigenvector of the Hessian; this is the general definition along the GE curves. Here for an intersection with the IB line, the corresponding eigenvalue is zero. We take this crossing as the indicator for the VB point of a new type. It shows additionally the property that the zero eigenvector, the gradient, is nearly orthogonal to the direction of the GE. So the GE touches a level line. The first condition is

$$\mathbf{H\,g = 0} \tag{10}$$

It is in contrast to a VRI point where the zero eigenvector is orthogonal to the gradient, Eq. (4). We find a fairly regular NT connection the SP with the minimum M over this VB point. It is at (x, y)=(0.56, 0.3) with

$\mathbf{g} = \begin{pmatrix} -1.35 \\ 0.47 \end{pmatrix}$, $\mathbf{H} = \begin{pmatrix} 0.04 & 0.13 \\ 0.13 & 0.35 \end{pmatrix}$ and $\mathbf{A} = \begin{pmatrix} 0.35 & -0.13 \\ -0.13 & 0.04 \end{pmatrix}$.

The search direction of the nonsingular NT is $\mathbf{g}=\mathbf{f}_{red}$=(−1.3533, 0.468). The Hessian matrix has the zero eigenvector being the gradient, and

$$\mathbf{A\,g} = \begin{pmatrix} -0.53 \\ 0.18 \end{pmatrix} = 0.39\;\mathbf{g} \neq \begin{pmatrix} 0 \\ 0 \end{pmatrix}.$$

A zero eigenvector of the Hessian is retained by the gradient, in this case. But 0.39 is the second eigenvalue of the direction orthogonal to the gradient. The value of the Branin vector is not zero which really shows that there is no

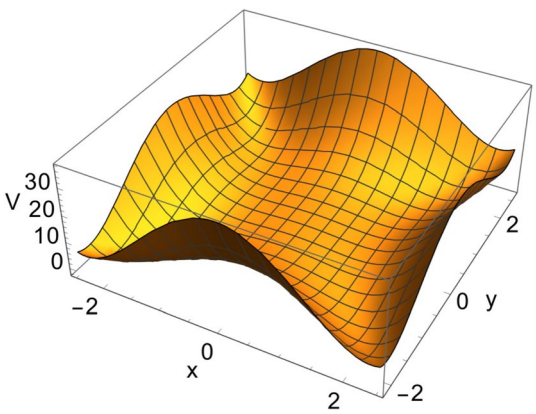

Fig. 3 3D representation of PES (8) for c=1. Only two uphill valleys remain. There are still two minima at the bottom, and the central SP also remains

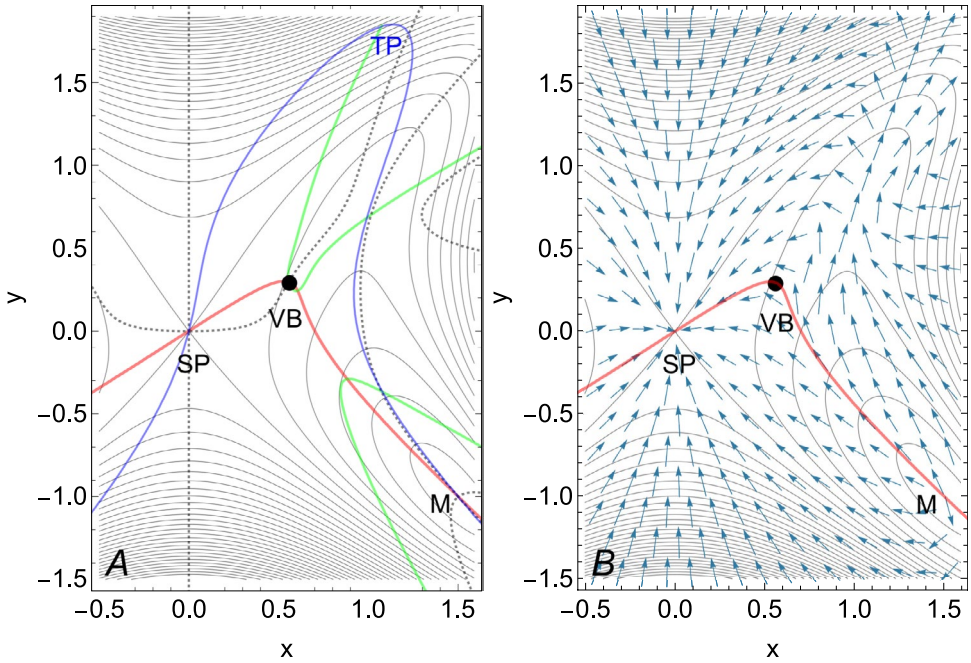

Fig. 4 **A:** Three kinds of curves are drawn on the PES for c=1. Red is the remainder of the former singular NT through the VB point, black dashed are the GE curves, and green are the IB lines. The blue curve is an ordinary regular NT. **B:** Vector field of Branin Eq. (2). The VB point is embedded in a nice flow of regular NTs

'normal' VRI point from the point of view of NTs. This is also an indication that such cases cannot be determined by the VRI finding method using the condition **A g=0** [51, 52]. Additionally, also μ of definition (6) does not change its sign; thus, it does not indicate the VRI point. Nevertheless, the GE crosses the IB line and has there the special eigenvalue $\lambda = 0$. We name this VB point for its crossing only by a GE. No bifurcation of a reaction trajectory takes place here. The condition $\mathbf{H}\,\mathbf{g} = \mathbf{0}$, at the other hand, is the criterion for an optimal barrier breakdown point (oBBP) in mechanochemistry [34–36]. But that is another story. The neighboring GE going uphill in the right valley ground intersects two times an IB line. However, the gradient there points in direction of the GE, not orthogonal to it. For the given VB point, it is more appropriate to use the GE being between the two bifurcating valleys.

With the blue NT in Fig. 4a we add a regular NT beginning at minimum M and initially following the valley uphill. It shows a turning point (TP) high in the PES mountains where the energy reaches a maximum, and it returns as a regular connection to the only remaining SP at point (0, 0). Its search direction is $\mathbf{f}_{blue}$=(−0.53, 1.11). The blue NT is an indication of the reason why this special VB point is useless for chemistry: The valley at the right-hand side is a 'dead' valley without a further TS and minimum. There cannot be a stable chemical structure. On the right sight of the PES, only one minimum and one SP exist. Every NT starting in the right minimum has to find its way to the central SP. There are no other stationary points, so the NT through the VB point must also be 'regular.' There is no target for it to bifurcate to. The entire right half-plane is one reaction channel [70]. The VB point exists but the index theorem acts that the VB does not disturb the channel of regular NTs.

Note that the NT through the VB crosses nearby the IB line a second time in the vicinity. We do not select the special NT with a single, tangential touch of the IB line for the definition of this new type of VB points.

In Fig. 4b the vector field of the right-hand side of the Branin Eq. (2) is again included. The NTs flow around the VB point. Their hyperbolic contact at the VB point is lost.

3.3 Action of the index theorem for singular NTs

Index Theorem for NTs

Regular NTs connect stationary points with an index difference of one [6, 38, 42]. This will be violated by a singular NT.

Proof: see appendix 1.

Figure 5A represents a quasi-shoulder region of the former SP_{low} and the former minimum M_2 for parameter $c = 1.125$. The two branches of the singular NT to SP_{low} and to the minimum M_2 come close together. They form quasi-parallel branches. After the two stationary points, they continue and end in a TP. The four branches intersect at a small angle at the VRI point. However, the index theorem also applies here in its usual form. Stationary points are connected by regular NTs (not shown) and the singular NT connects with two branches the two SPs of index one, and with two other branches the two minima with index 0.

The situation changes further in panel B of Fig. 5 where we obtain a real shoulder point. We insert the pseudo-convexity index (6) $\mu = 0$ by black lines. Here the former SP_{low}

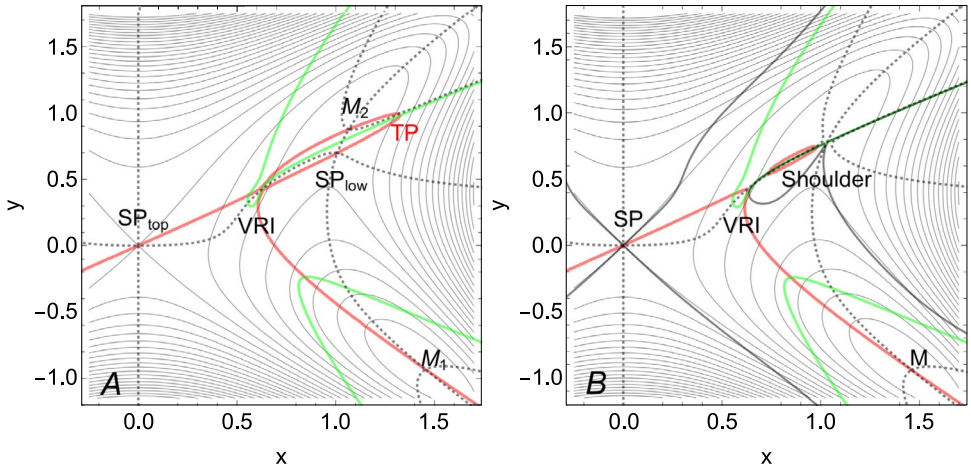

Fig. 5 A: PES (8) for c=1.125. The former low SP and the former minimum M_2 nearly merge and almost form a flat shoulder. The minimum M_1 is still at the bottom, and the central SP also remains. B: PES for c=1.11 which forms a PES with a shoulder point. Red is the rest of the singular NT through the VRI point, black dashed are GE curves, the pseudo-convexity index $\mu = 0$ are black lines, and green are the IB lines

and the former minimum M_2 have merged. The remaining point is a stationary point with a zero gradient and a zero eigenvector along the valley line. The PES is obtained by parameter $c = 1.11$. The shoulder is demonstrated by the GEs there, which do not cross as in stationary points but avoid a crossing near the former SP_{low}. Quasi-three branches of the singular NT remain from the VRI. It is the limiting case. The next step is then the case of Fig. 4 with c=1, where the character of the singular NT is lost, and where the connection to the former shoulder region also is finally lost.

Fig.6A shows an enlargement of the VRI region from Fig.5B. The black lines are the boundary of the pseudo-convexity (6) $\mu = 0$. In addition to the standard VRI point with a singular NT in red color through the dot symbol, a VB point also appears, at the cross, ×, where again the gradient is orthogonal to the GE direction. In contrast, at the plus + symbol, we find a crossing of GE and IB line with no orthogonal gradient direction to the GE. The point × is crossed by an ordinary NT in brown color. In contrast, three special curves meet at the + symbol: a GE, an IB, and the $\mu = 0$-line.

Here we have a loop of the singular NT, the former quasi-parallel branches to the shoulder. The point +, inside the loop, is the center of a family of compact NTs, called center NTs [38, 70]. One of these NTs is drawn in magenta color. NTs without stationary points are possible [68, 70]. We assume that they are not of deeper interest for chemical reasons. The VRIs are the most important definition, the first level in a hierarchy of valley bifurcations, so to speak. The VB of species × forms the second level, which we should use if no VRI is there.

For comparison, we include still two neighboring NTs to the singular one, in Fig. 6b, in blue color. The dashed NT follows the search direction (-1, 0.36), it bypasses the VRI region on the right. The pure blue NT follows the (-1, 0.3) direction and runs to the SP at the left-hand side of the VRI.

Note that there is a parameter c nearby at ≈1.10697 where the VRI point and the point at the + symbol merge. Such a special singularity is called a cusp type [70]. For smaller values of c, the VB point lefts over only.

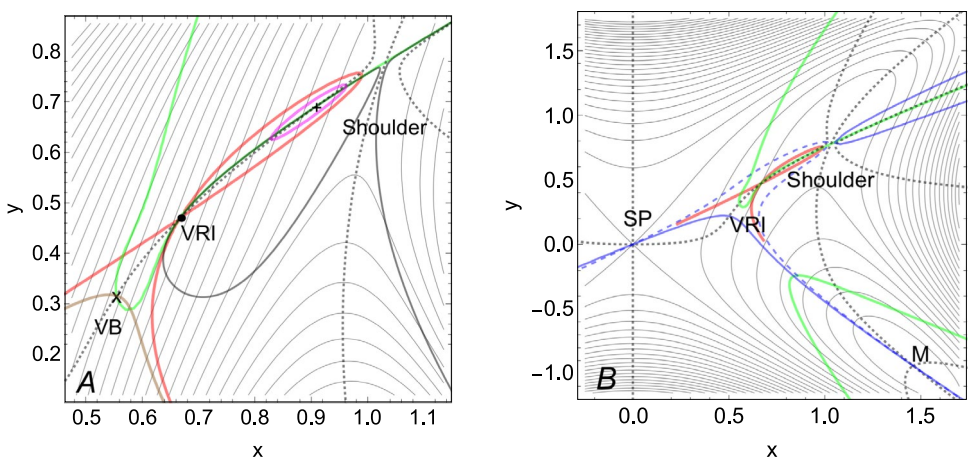

Fig. 6 A: Enlargement of Fig.5B with a VB point, x, and a VRI point, •, see text. B: Two regular NTs in blue are additionally included in Fig. 5b, see text

4 Discussion

An important model for a reaction coordinate in chemistry is the steepest descent from SP, the intrinsic reaction coordinate (IRC) [29, 30]. In case of a symmetric PES and a totally symmetric axis through the SP [71–73], the IRC can cross a possible VRI point on this downhill path [31, 74–76]. However, on an asymmetric PES, the VRI is usually not located on the steepest descent from the SP [9, 77, 78]. There, any other reaction trajectory could bifurcate off from the IRC [79]. It is incorrect that the IRC splits itself at the VRI point [80, 81]. The IRC can split only at stationary points, where the gradient is zero, and where different directions for the further travel downhill can open. SPs are the singular points of the steepest descent trajectories. Analogous to NTs near VRI points, these trajectories follow hyperbolic curves around SPs.

One way out is a dynamical approach by many trajectories over the entrance SP region [19, 82–89]. This method contrasts with static models of a reaction pathway for IRC, NT, or GE. Localization through two sets of dynamical trajectories bifurcating near the VRI point is one way of a certain determination of the VRI point and product selectivity. Although dynamic trajectories can theoretically identify the VRI, this approach is unrealistic and hardly feasible in a real system. According to the ergodic hypothesis [90], a single trajectory could explore the entire configuration space if it moves forever in phase space, including the VRI. However, this is a multidimensional problem, and the growth of dimensions is proportional to the number of atoms involved. Finding a specific outcome amidst such complexity is highly unrealistic.

The other possibility is the calculation of GEs and a singular NT to precisely locate the VRI. Of course, this exceptional VB point of case $c = 1$ of Fig. 4 cannot be detected using dynamical trajectories or a singular NT.

One can speculate that such VB points also exist on other, older known PES. Because 'dead' valleys often exist. For example the well-known Müller-Brown PES [91] has such a valley on the left-hand side, and no singular NT crosses it [68, 69]. In contrast, here also crosses a GE the IB line at point $(x, y)=(-1.09771, 0.6487)$ and the gradient is also nearly orthogonal to the GE direction, compare Fig. 7. This point we propose for a VB indicator. The most left GE of the left valley ground intersects also the IB line. There the gradient points in direction of the valley ground, which also the GE follows. For the VB point, it is more appropriate to use the GE being more between the two bifurcating valleys.

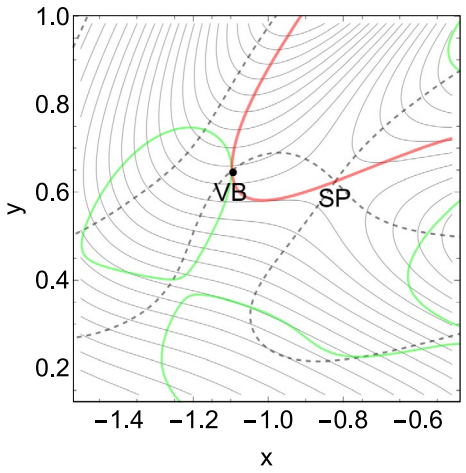

Fig. 7 MB surface with proposed VB at the branching of the left global valley. Red is a regular NT, green are the IB lines

5 Conclusion

We use Newton trajectories (NT), gradient extremals (GE) and lines of the boundaries of the Hessian index (IB) with Det(**H**)=0 to explore the region of a VRI or a VB point. Long known are VRI points where a singular NT bifurcates. Its side branches form static models of a reaction path bifurcation. They can serve for models of trajectories to two different products.

By changing the parameter c of the PES of Ref. [33] we obtain a VB region with the special case of no singular NT. In the special situation of the VB point of this PES (8) with parameter c=1, the usual criteria for a VRI point, Eqs. (4) for NTs and (6) for GEs do not work appropriately. In contrast, a GE only crosses an IB line and the gradient is orthogonal to the GE direction. This point we can accentuate for a VB point. One eigenvalue of the Hessian is zero, and the corresponding eigenvector is the gradient. Thus, it holds Eq. (10). The nature of the PES of this case is that the one bifurcating valley is a 'dead' valley with no further stationary points. A 'dead' valley may be uninteresting for a chemical reaction, but it can be the basis for a vibration mode. The branching takes place without a ridge forming between the two new valleys. The 'next ridge' is the ridge that crosses the SP of the new side valley.

VRI and VB points form a hierarchy. The usual VRI points have been known for a long time. The VB points form a weaker level, which we should assign if a usual VRI is missing.

Appendix 1: Proof of the Index Theorem

We follow references [68, 92, 93]. The Branin Eq. (2) is the desingularized continuous Newton equation. For the minus sign, it converges to a stationary point with an even index, i.e., a minimum with index zero as in the Newton–Raphson method. For plus sign, however, it converges to a stationary point with an odd index, compare Figs.2 and 4b. It can be developed with a Taylor approach for the gradient

$$\mathbf{g}(\mathbf{x}) \approx \mathbf{g}(\mathbf{x_0}) + \frac{\partial \mathbf{g}}{\partial \mathbf{x}}(\mathbf{x_0})\,(\mathbf{x}-\mathbf{x_0})$$

and for zero gradient at $\mathbf{x_0}$ it is

$$= \mathbf{H}(\mathbf{x_0})\,(\mathbf{x}-\mathbf{x_0})\,.$$

Eq. (2) looks then

$$\frac{d\mathbf{x}}{dt} \approx -\,\mathbf{A}(\mathbf{x})\mathbf{H}(\mathbf{x_0})\,(\mathbf{x}-\mathbf{x_0}) \;\approx -Det(\,\mathbf{H}(\mathbf{x_0}))\,(\mathbf{x}-\mathbf{x_0})\,,$$

and this is attractive for even index, but repulsive for odd index of $\mathbf{H}(\mathbf{x_0})$.

For illustration, Fig. 8 shows a test surface with three types of stationary points. Regular NTs from the maximum at (0, 0.5) only lead to SPs of index one, and so on. Thus starting near of one of the two kinds of stationary points, an NT (with corresponding ± change) will lead to the other kind, by an index difference of one. This rule can only be violated by a VRI point on a singular NT.

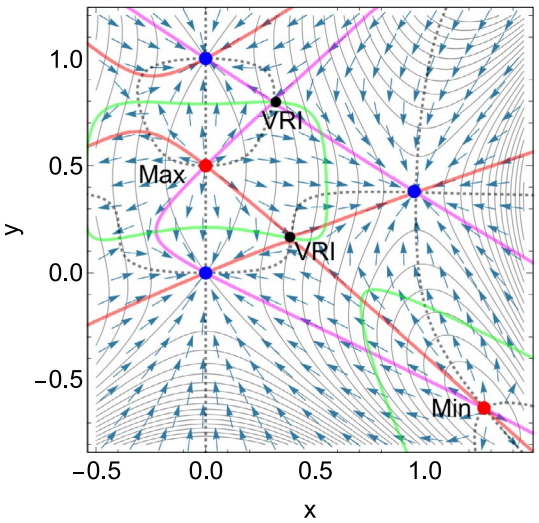

Fig. 8 PES (8) with c=2 now with an SP of index two, a maximum. Red points are stationary points with even indices, the minimum and the maximum, while blue points are three SPs of index one, three TSs. Two singular NTs cross two VRI points (black), one NT is red colored, and one NT is in magenta

Appendix 2: Discussion of GE bifurcations

On a symmetric PES, a valley GE can bifurcate and indicate the branching of the PES [67]. Which criterion we apply may depend on the problem to be solved.

Now we study the avoided crossing of GEs, which is the usual behavior of GEs on an asymmetric PES, see Fig. 9. An artificial 2D PES [63] is

$$V(x,y) = x\,y\,(y-x) + 1.15\,x^2 + 2\,y - 3\,.$$

Doted curves represent three GEs, the two red lines are the singular NT, and the green elliptic curve is the IB line. In the center is the intersection of the GE from left to right and the red singular NT. It is a common VRI point. The GEs themselves only cross at the SPs. The aim of recognizing a VB by the crossing of the GEs would therefore fail here.

However, a valley bifurcation before the VRI can be assumed, below the level of the SPs, which is indicated by an additional VB point shown. It is the intersection of the left GE with the IB line where the gradient is orthogonal to the GE.

Appendix 3: Representation of NTs and of GEs

2D PES with NTs [68]

In 2D toy examples, NTs can easily be represented by a graphical rule. It applies in two dimensions that the orthogonal direction to the force direction

$\mathbf{f}=\binom{f_1}{f_2}$ is unique the direction $\mathbf{f}^{\perp} = (-f_2, f_1)\,.$

Then condition (1) that $\mathbf{f} \,||\, \mathbf{g}$ is the zero of the scalar product

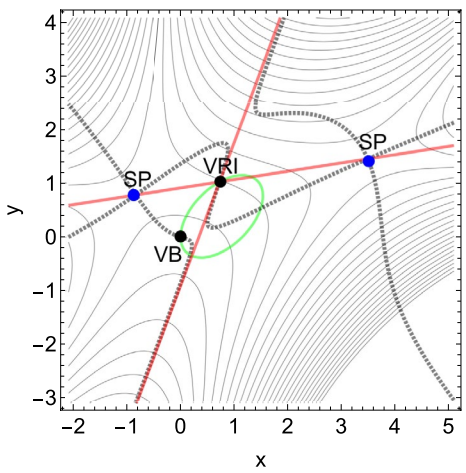

Fig. 9 PES with avoided crossings of GEs (black dashes). Blue points are SPs. Two branches of the singular NT (red) cross at the VRI point a GE. An additional VB point is included, see text

$$\mathbf{f}^{\perp}\,\mathbf{g} = \mathbf{0}\,.$$

In Mathematica, one can represent the corresponding NT by

```
ContourPlot[-g1[x,y] f2[x,y] + g2[x,y] f1[x,y],{x,-2,2},{y,-2,2}, ContourShading→False, Contours→{0.0}]
```

2D PES with GEs

In analogy to NTs, also GEs can easily be represented by a graphical rule in 2D examples. It applies in two dimensions that the orthogonal direction to the gradient direction $\mathbf{g}=\binom{g_1}{g_2}$ is unique the direction $\mathbf{g}^{\perp} = (-g_2, g_1)$.

Then condition (5) means that $\mathbf{H}\,\mathbf{g} \,||\, \mathbf{g}$, and this is again the zero of the scalar product

$$\mathbf{g}^{\perp}\,\mathbf{H}\,\mathbf{g} = \mathbf{0}\,.$$

One can display the corresponding GE in a graphic program analogously to above.

Acknowledgements We thank a reviewer for suggesting Fig.6A, Fig.9, and for many questions and important comments. JMB thanks the Spanish Structures of Excellence María de Maeztu Program, Grant CEX2021-001202-M, and the Agència de Gestió d'Ajuts Universitaris i de Recerca of Generalitat de Catalunya, Projecte 2021 SGR 00354. GHHCh acknowledges support from the Max-Planck Gesellschaft via the MPI-PKS visitors program.

Author Contributions WQ, HHGCh, and JMB contributed equally.

Funding Open Access funding enabled and organized by Projekt DEAL.

Data Availability All relevant data are included in the paper. Further data can be obtained from WQ.

Declarations

Conflict of interest We declare that we have no affiliation with or involvement in any organization that has a financial interest in the subject matter or materials discussed herein.

References

1. Stewart I (1981) Applications of catastrophe theory to the physical sciences. Physica D 2:245–305
2. Crawford JD (1991) Introduction to bifurcation theory. Rev Mod Phys 63:991–1037
3. Valtazanos P, Ruedenberg K (1986) Bifurcations and transition states. Theor Chim Acta 69:281–307
4. Baker J, Gill PMW (1988) An algorithm for the location of branching points on reaction paths. J Comput Chem 9:465–475
5. Yamamoto N, Bernardi F, Bottoni A, Olivucci M, Robb MA, Wilsey S (1994) Mechanism of carbene formation from the excited states of diazirine and diazomethane: An MC-SCF study. J Am Chem Soc 116:2064–2074
6. Quapp W, Hirsch M, Heidrich D (1998) Bifurcation of reaction pathways: the set of valley ridge inflection points of a simple three-dimensional potential energy surface. Theor Chem Acc 100(5/6):285–299
7. Margalef-Roig J, Miret-Artes S, Toro-Labbe A (2000) Characterization of elementary chemical reactions from bifurcation theory. J Phys Chem A 104:11589–11592
8. Quapp W, Hirsch M, Heidrich D (2004) An approach to reaction path branching using valley-ridge inflection points of potential energy surfaces. Theor Chem Acc 112:40–51
9. Suhrada CP, Selcuki S, Nendel N, Cannizzaro C, Houk KN, Rissing P-J, Baumann D, Hasselmann D (2005) Dynamic effects on [3,3] and [1,3] shifts of 6-methylenebicyclo[3.2.0]hept-2-ene. Angew. Chem., Int. Ed. 44, 3548–3552
10. Goldsmith BR, Sanderson ED, Bean D, Peters B (2013) Isolated catalyst sites on amorphous supports: A systematic algorithm for understanding heterogeneities in structure and reactivity. J Chem Phys 138:204105
11. Windhorn L, Yeston JS, Witte T, Fuss W, Motzkus M, Proch D, Kompa KL, Moore CB (2003) Getting ahead of IVR: A demonstration of mid-infrared induced molecular dissociation on a sub-statistical time scale. J Chem Phys 119:641–644
12. Michel L (1980) Symmetry defects and broken symmetry. Config Hidden Symmetry Rev Mod Phys 52:617–651
13. Kraus WA, DePristo AE (1986) Reaction dynamics on bifurcating potential energy surfaces. Theoret Chim Acta 69:309–322
14. Bakken V, Danovich D, Shaik S, Schlegel HB (2001) A single transition state serves two mechanisms: An ab initio classical trajectory study of the electron transfer and substitution mechanisms in reactions of ketyl radical anions with alkyl halides. J Am Chem Soc 123:130–134
15. Limanto J, Khuong KS, Houk KN, Snapper ML (2003) Intramolecular cycloadditions of Cyclobutadiene with Dienes: Experimental and computational studies of the competing (2 + 2) and (4 + 2) modes of reaction. J Am Chem Soc 125:16310–16321
16. Lasorne B, Dive G, Lauvergnat D, Desouter-Lecomte M (2003) Wave packet dynamics along bifurcating reaction paths. J Chem Phys 118(13):5831–5840
17. Zheng J, Papajak E, Truhlar DG (2009) Phase space prediction of product branching ratios: Canonical competitive nonstatistical model. J Am Chem Soc 131(43):15754–15760
18. Rehbein J, Carpenter BK (2011) Do we fully understand what controls chemical selectivity? Phys Chem Chem Phys 13:20906–20922
19. Ohashi M, Liu F, Hai Y, Chen M, Tang M-C, Yang Z, Sato M, Watanabe K, Houk KN, Tang Y (2017) SAM-dependent enzyme-catalysed pericyclic reactions in natural product biosynthesis. Nature 549:502–506
20. Ge L, Li S, George TF, Sun X (2013) A model of intrinsic symmetry breaking. Phys Lett A 377:2069–2073
21. Sanchez-Galvez A, Hunt P, Robb MA, Olivucci M, Vreven T, Schlegel HB (2000) Ultrafast radiationless deactivation of organic dyes: evidence for a two-state two-mode pathway in polymethine cyanines. J A Chem Soc 122:2911–2924
22. Wang Z, Hirschi JS, Singleton DA (2009) Recrossing and dynamic matching effects on selectivity in a Diels-Alder reaction. Angew Chem Int Ed Engl 48(48):9156–9159

23. Chuang H-H, Tantillo DJ, Hsu C-P (2020) Construction of two-dimensional potential energy surfaces of reactions with post-transition-state bifurcations. J Chem Theory Computat 16(7):4050–4060
24. Çelebi-Ölçüm N, Ess DH, Aviyente V, Houk KN (2007) Lewis acid catalysis alters the shapes and products of bis-pericyclic Diels-Alder transition states. J Am Chem Soc 129:4528–4529
25. Ess DH, Wheeler SE, Iafe RG, Xu L, Çelebi-Ölçüm N, Houk KN (2008) Bifurcations on potential energy surfaces of organic reactions. Angew Chem Int Ed 47:7592–7601
26. Lee S, Goodman JM (2020) Rapid route-finding for bifurcating organic reactions. J Am Chem Soc 142(20):9210–9219
27. Katsanikas M, Garcia-Garrido VJ, Agaoglou M, Wiggins S (2020) Phase space analysis of the dynamics on a potential energy surface with an entrance channel and two potential wells. Phys Rev E 102:012215
28. Crossley R, Agaoglou M, Katsanikas M, Wiggins S (2021) From Poincaré maps to Lagrangian descriptors: The case of the valley ridge inflection point potential. Regul Chaot Dyn 26:147–164
29. Fukui K (1970) A formulation of the reaction coordinate. J Phys Chem 74:4161–4163
30. Quapp W, Heidrich D (1984) Analysis of the concept of minimum energy path on the potential energy surface of chemically reacting systems. Theor Chim Acta 66:245–260
31. Taketsugu T, Yanai T, Hirao K, Gordon MS (1998) Dynamic reaction path study of SiH4+F- → SiH4F- and the Berry pseudorotation with valley-ridge inflection. J. Molec. Struc.: THEOCHEM 451(1-2), 163–177
32. Maeda S, Harabuchi Y, Ono Y, Taketsugu T, Morokuma K (2015) Intrinsic reaction coordinate: Calculation, bifurcation, and automated search. Int J Quant Chem 115:258–269
33. Su H, Wang H, Zhang L, Zhao J, Zheng X. Improved high-index saddle dynamics for finding saddle points and solution landscape. arXiv 2502.03694v2, 1–19 (2025)
34. Quapp W, Bofill JM (2016) A contribution to a theory of mechanochemical pathways by means of Newton trajectories. Theoret Chem Acc 135(4):113
35. Quapp W, Bofill JM, Ribas-Arino J (2018) Towards a theory of mechanochemistry- simple models from the very beginning. Int J Quant Chem 118:25775
36. Quapp W, Bofill JM (2024) Theory and examples of catch bonds. J Phys Chem B 128(17):4097–4110
37. Branin FH (1972) Widely convergent methods for finding multiple solutions of simultaneous nonlinear equations. IBM J Res Develop 16:504–522
38. Jongen HT, Jonker P, Twilt F (2000) Nonlinear Optimization in Finite Dimensions. Kluwer Academic Publ, Dordrecht
39. Bofill JM (1994) Updated Hessian matrix and the restricted step method for locating transition structures. J Computat Chem 15:1–11
40. Anglada JM, Besalú E, Bofill JM, Rubio J (1999) Another way to implement the Powell formula for updating Hessian matrices related to transition structures. J Math Chem 25:85–92
41. Hratchian HP, Schlegel HB (2005) Using Hessian updating to increase the efficiency of a Hessiian based predictor-corrector relation path following method. J Chem Theory Computat 1:61
42. Bofill JM, Quapp W (2011) Variational nature, integration, and properties of the Newton reaction path. J Chem Phys 134:074101
43. Hirsch M, Quapp W, Heidrich D (1999) The set of valley-ridge inflection points on the potential energy surface of the water molecule. Phys Chem Chem Phys 1:5291–5299
44. Quapp W, Melnikov V (2001) The set of valley ridge inflection points on the potential energy surfaces of H_2S, H_2Se and H_2CO. Phys Chem Chem Phys 3:2735–2741
45. Bofill JM, Quapp W (2013) Analysis of the valley-ridge inflection points through the partitioning technique of the Hessian eigenvalue equation. J Math Chem 51:1099–1115
46. Quapp W, Bofill JM, Aguilar-Mogas A (2011) Exploration of cyclopropyl radical ring opening to allyl radical by Newton trajectories: Importance of valley-ridge inflection points to understand the topography. Theor Chem Acc 129:803–821
47. Quapp W (2015) Can we understand the branching of reaction valleys for more than two degrees of freedom? J Math Chem 54:137–148
48. COLUMBUS: program system. https://columbus-program-system.gitlab.io/ columbus/ (2023)
49. Quapp W (2011) Program for unsymmetric valley-ridge inflection points. www.math.uni-leipzig.de/~quapp/SkewVRIs.html
50. Quapp W (2024) Mathematica notebook for catch bond calculations. https://community.wolfram.com/groups/-/m/t/3167380 , **Wolfram**
51. Quapp W, Schmidt B (2011) An empirical, variational method of approach to unsymmetric valley-ridge inflection points. Theor Chem Acc 128:47–61
52. Schmidt B, Quapp W (2012) Search of manifolds of nonsymmetric valley-ridge inflection points on the potential energy surface of HCN. Theor Chem Acc 132:1305–1313
53. Garcia-Garrido VJ, Wiggins S (2021) The dynamical significance of valley-ridge inflection points. Chem Phys Lett 781:138970
54. Gonzalez J, Gimenez X, Bofill JM (2002) A reaction path Hamiltonian defined on a Newton path. J Chem Phys 116:8713–8722
55. Quapp W (2005) A growing string method for the reaction pathway defined by a Newton trajectory. J Chem Phys 122:174106
56. Konda SSM, Brantley JM, Bielawski CW, Makarov DE (2011) Chemical reactions modulated by mechanical stress: Extended Bell theory. J Chem Phys 135:164103
57. Cardozo TM, Galliez AP, Borges I Jr, Plasser F, Aquino AJA, Barbatti M, Lischka H (2019) Dynamics of benzene excimer formation from the parallel-displaced dimer. Phys Chem Chem Phys 21:13916–13924
58. Barkan CO, Bruinsma RF (2024) Topology of molecular deformations induces triphasic catch bonding in selectin-ligand bonds. Proc Natl Acad Sci 121:2315866121
59. Hopper N, Rana R, Sidoroff F, Cayer-Barrioz J, Mazuyer D, Tysoe WT (2025) Activation volumes in tribochemistry; what do they mean and how to calculate them? Tribol Lett 73:40
60. Quapp W (2007) Finding the transition state without initial guess: the growing string method for Newton trajectory to isomerisation and enantiomerisation reaction of alanine dipeptide and poly(15) alanine. J Computat Chem 28:1834–1847
61. Hoffmann DK, Nord RS, Ruedenberg K (1986) Gradient extremals. Theor Chim Acta 69:265–280
62. Sun J-Q, Ruedenberg K (1993) Gradient extremals and steepest descent lines on potential energy surfaces. J Chem Phys 98:9707–9714
63. Quapp W (1989) Gradient Extremals and Valley Floor Bifurcation on Potential Energy Surfaces. Theoret Chim Acta 75:447–460
64. Schlegel HB (1992) Following gradient extremal paths. Theor Chim Acta 83:15–20
65. Hirsch M, Quapp W (2004) Reaction pathways and convexity of the potential energy surface: Application of Newton trajectories. J Math Chem 36:307–340
66. Bofill JM, Quapp W, Caballero M (2012) The variational structure of gradient extremals. J Chem Theory Computat 8:927–935
67. Quapp W, Hirsch M, Heidrich D (2000) Following the streambed reaction on potential energy surfaces: a new robust method. Theor Chem Acc 105:145–155

68. Hirsch M (2004) Zum Reaktionswegcharakter von Newtontrajektorien (in german). Dissertation, University Leipzig, Faculty of Chemistry and Mineralogy
69. Quapp W, Bofill JM (2018) Mechanochemistry on the Müller-Brown surface by Newton trajectories. Int. J. Quant. Chem. 118, 25522
70. Hirsch M, Quapp W (2004) Reaction Channels of the Potential Energy Surface: Application of Newton Trajectories. J. Molec. Struct., THEOCHEM 683(1-3), 1–13
71. Pechukas P (1976) On simple saddle points of a potential surface, the conservation of nuclear symmetry along paths of steepest descent, and the symmetry of transition states. J Chem Phys 64:1516–1521
72. Bone RGA (1992) Deducing the symmetry operations generated at the transition state. Chem Phys Lett 193:557–564
73. Schaad LJ, Hu J (1998) Symmetry rules for transition structures in degenerate reactions. J Am Chem Soc 120:1571–1580
74. Minyaev RM, Wales DJ (1994) Gradient line reaction path of HF addition to ethylene. Chem Phys Lett 218(5–6):413–421
75. Harabuchi Y, Taketsugu T (2011) A significant role of the totally-symmetric valley-ridge inflection point in the bifurcating reaction pathway. Theoret Chem Acc 130:305–315
76. Zhou C, Birney DM (2002) Sequential transition states and the valley-ridge inflection point in the formation of a semibullvalene. Organic Lett 4:3279–3282
77. Debbert SL, Carpenter BK, Hrovat DA, Borden WT (2002) The iconoclastic dynamics of the 1,2,6-heptatriene rearrangement. J Am Chem Soc 124:7896–7897
78. Pomerantz A, Camden JP, Chioiu AS, Ausfelder F, Chawia N, Hase WL, Zare RN (2005) Reaction products with internal energy beyond the kinematic limit result from trajectories far from the minimum energy path: An example from H+HBr → H_2 + Br. J Am Chem Soc 127(47):16368–16369
79. Okada K, Sugimoto M, Saito K (1994) A reaction-path dynamics approach to the thermal unimolecular decomposition of acetaldoxime. Chem Phys 189:629–636
80. Shustov GV, Rauk A (1998) Mechanism of dioxirane oxidation of CH bonds, application to homo- and heterosubstituted alkanes as a model of the oxidation of peptides. J Organic Chem 63(16):5413–5422
81. Carpenter BK, Harvey J, Glowacki D (2015) Prediction of enhanced solvent-induced enantioselectivity for a ring opening with a bifurcating reaction path. Phys Chem Chem Phys 17:8372–8381
82. Mann DJ, Hase WL (2002) Ab initio direct dynamics study of cyclopropyl radical ring-opening. J Am Chem Soc 124:3208–3209
83. Taketsugu T, Kumeda Y (2001) An ab initio direct-trajectory study of the kinetic isotope effect on the bifurcating reaction. J Chem Phys 114:6973–6982
84. Gonzalez-Lafont A, Moreno M, Lluch JM (2004) Variational transition state theory as a tool to determine kinetic selectivity in reactions involving a valley-ridge inflection point. J Am Chem Soc 126:13089–13094
85. Ussing BR, Hang C, Singleton DA (2006) Dynamic effects on the periselectivity, rate, isotope effects, and mechanism of cycloadditions of ketenes with cyclopentadiene. J Am Chem Soc 128:7594–7607
86. Thomas JB, Waas JR, Harmata M, Singleton DA (2008) Control elements in dynamically determined selectivity on a bifurcating surface. J Am Chem Soc 130:14544–14555
87. Yamamoto Y, Hasegawa H, Yamataka H (2011) Dynamic path bifurcation in the Beckmann reaction: Support from kinetic analyses. J Org Chem 76:4652–4660
88. Hong YJ, Tantillo DJ (2014) Biosynthetic consequences of multiple sequential post-transition-state bifurcations. Nat Chem 6:104–111
89. Kong W-Y, Hu Y, Guo W, Potluri A, Schomaker JM, Tantillo DJ (2025) Synthetically relevant post-transition state bifurcation leading to diradical and zwitterionic intermediates: Controlling nonstatistical kinetic selectivity through solvent effects. J. Am. Chem, Soc
90. Boltzmann L (1898) Vorlesungen über Gastheorie. J. A. Barth, Leipzig
91. Müller K, Brown LD (1979) Location of saddle points and minimum energy paths by a constrained simplex optimisation procedure. Theor Chim Acta 53:75–93
92. Diener I (1991) Globale Aspekte des kontinuierlichen Newtonverfahrens. University Göttingen, Göttingen, Habilitation
93. Diener I (1995) Trajectory methods in global optimization. In: Horst R, Pardalos PM (eds) Handbook of Global Optimization, vol 2. Nonconvex Optimization and Its Applications. Springer, US, pp 649–668